

## A Study of the Magnetic Superexchange Interactions in the Solid-Solution Series $\text{Ca}_x\text{Sr}_{1-x}\text{RuO}_3$ by Ruthenium-99 Mössbauer Spectroscopy

TERENCE C. GIBB, ROBERT GREATREX,  
NORMAN N. GREENWOOD,\* DAVID C. PUXLEY, AND  
KENNETH G. SNOWDON

*Department of Inorganic and Structural Chemistry,  
The University of Leeds, Leeds LS2 9JT, England*

Received November 15, 1973

Ruthenium-99 Mössbauer spectroscopy has been used to examine magnetic superexchange interactions in the distorted perovskite solid-solutions  $\text{Ca}_x\text{Sr}_{1-x}\text{RuO}_3$  ( $x = 0.1, 0.2, 0.3, 0.4,$  and  $0.5$ ). The end members of this series also have a slightly distorted perovskite structure but  $\text{CaRuO}_3$  is Curie-Weiss paramagnetic, with only a single-line Mössbauer spectrum, whereas  $\text{SrRuO}_3$  is ferromagnetic and shows a broad well-resolved hyperfine pattern. For  $x \leq 0.2$  a substantial proportion of the ruthenium atoms experience a magnetic flux density (hyperfine magnetic field) close to 35T, but inward collapse of the spectrum suggests that an increasing proportion of ruthenium atoms experience smaller flux densities. For samples with  $x \leq 0.3$  there is an intense central "paramagnetic" component which increases rapidly with increasing  $x$ . The observed behaviour is incompatible with a conventional localized electron structure but can be interpreted satisfactorily on a collective electron model in which the average spin moment and hence the magnetic flux density at any given ruthenium atom is proportional to the strength of the exchange interactions with the six nearest-neighbour ruthenium atoms. The results imply that the greater electron-pair acceptor strength (Lewis acidity) of  $\text{Ca}^{2+}$  compared to  $\text{Sr}^{2+}$  results in a more effective competition with ruthenium for the oxygen anion orbitals involved in the superexchange interaction. It appears that, for a ruthenium to have a coupled spin-moment, it must have at least two exchange interactions through cube faces containing at least three strontium atoms. Possible origins of the reduced magnetic moment of  $\text{SrRuO}_3$  are discussed and it is suggested that the latter probably stems from spin-canting rather than from partial overlap of spin-up and spin-down bands.

### Introduction

Our interest in the mixed phase  $\text{Ca}_x\text{Sr}_{1-x}\text{RuO}_3$  stems directly from earlier observations of the striking difference in magnetic properties of the end-members  $\text{SrRuO}_3$  and  $\text{CaRuO}_3$  (1).

$\text{SrRuO}_3$  is an orthorhombic distorted perovskite with cell dimensions  $a = 553.19$ ,  $b = 557.24$ ,  $c = 784.96$  pm. The material is also a metallic conductor with  $\rho \sim 2.75 \times 10^{-4}$  ohm cm at 300°K (2). In the paramagnetic

state the magnetic moment is about  $2.65 \mu_B$  compared to a calculated value of  $2.83 \mu_B$  for  $S = 1$  on the spin-only formula. The oxide is ferromagnetic below  $T_C = 160^\circ\text{K}$  with a saturation magnetisation of ca.  $20 \text{ emu g}^{-1}$  ( $= 1.6 \text{ m}^3 \text{ g}^{-1} = 377 \text{ m}^3 \text{ mole}^{-1}$  in SI units) leading to  $\mu = 0.85 \mu_B$  per Ru (3). Possible origins of the reduced moment of  $\text{SrRuO}_3$  have been discussed in the literature (3-5) and these are reviewed later in this paper in the light of our own results.

$\text{CaRuO}_3$  is also an orthorhombic distorted perovskite with  $a = 552.89$ ,  $b = 535.56$ ,  $c = 766.01$  pm (2). It follows a Curie-Weiss law

\* Author to whom correspondence should be addressed.

at high temperatures with a negative Weiss constant (3). Goodenough *et al.* gave  $\mu_{\text{eff}} = 2.97 \mu_{\text{B}}$  and indicated a Néel temperature of  $110 \pm 10^\circ\text{K}$  (4, 5) but our recent Mössbauer data at  $4.2^\circ\text{K}$  (1) and neutron diffraction data (6) show no evidence of magnetic ordering. The conductivity is similar to that of  $\text{SrRuO}_3$  ( $\sim 2.5 \times 10^{-4}$  ohm cm at  $300^\circ\text{K}$ ) but shows no anomalies down to  $4.2^\circ\text{K}$ , in contrast to  $\text{SrRuO}_3$  which has an anomaly at the Curie temperature (2).

It has been said that the similar conduction behaviour argues against any large differences in carrier mobility, conduction band width, and by implication degree of covalent Ru–O  $\pi$ -bonding in these two oxides (2), although we are led to doubt the latter point on the basis of our own results. The high conductivity of these oxides, coupled with their Curie–Weiss paramagnetism (above  $T_{\text{C}}$  in the case of  $\text{SrRuO}_3$ ) rather than Pauli paramagnetism of a true metal, imply that the  $4d$  electrons of the ruthenium atoms are itinerant but still comparatively “tightly bound” to the metal. The two compounds are closely related both chemically and structurally and it is therefore particularly surprising that there should be this striking difference in magnetic properties. A study of the solid-solution  $\text{Ca}_x\text{Sr}_{1-x}\text{RuO}_3$  was therefore undertaken to probe these magnetic interactions more deeply.

## Experimental

The end members  $\text{SrRuO}_3$  and  $\text{CaRuO}_3$  were prepared by published methods (7, 8) from stoichiometric proportions of ruthenium metal and the alkaline–earth carbonates. The intermediate members of this series with  $x = 0.1, 0.2, 0.3, 0.4,$  and  $0.5$  were prepared as single-phase materials using the method of Longo (9, 10). This involved heating stoichiometric amounts of strontium carbonate and calcium carbonate together with a 25% excess of ruthenium dioxide (to allow for loss by evaporation) in a platinum crucible for 24 hr at  $1200^\circ\text{C}$ . By this time the X-ray patterns indicated no trace of excess  $\text{RuO}_2$  and showed clear sharp lines from phases isostructural with the end member  $\text{SrRuO}_3$  ( $x = 0$ ).

The products were examined with a Phillips powder diffractometer using  $\text{CuK}_\alpha$  radiation ( $\lambda = 154.18$  pm). Magnetic susceptibilities were measured with a variable temperature Gouy balance in the temperature range  $85$ – $300^\circ\text{K}$ . A vibrating sample magnetometer was also used to study the more highly magnetic materials  $\text{SrRuO}_3$  and  $\text{Ca}_{0.5}\text{Sr}_{0.5}\text{RuO}_3$ . The Mössbauer spectrometer embodied an MVT3 transducer, an MD3 drive amplifier, and an MFG3 waveform generator from Elscint Ltd., Israel. These units were coupled with a Northern Scientific Inc. NS630 multi-channel analyser. The radioactive source was made at the A.E.R.E., Harwell and consisted of  $\sim 10$  mCi of  $^{99}\text{Rh}$ , chemically extracted from the products of a  $^{99}\text{Ru} (d, 2n) ^{99}\text{Rh}$  reaction and incorporated into a ruthenium metal matrix. Both the source and absorber were held at  $4.2^\circ\text{K}$  in a liquid helium cryostat, which was also manufactured by Elscint Ltd. All spectra were analysed by computer fitting techniques to be described later, and were calibrated using the spectrum of an iron foil at room temperature. The spectrum of ruthenium metal at  $4.2^\circ\text{K}$  was used as the reference zero of velocity.

## Crystallographic Data

The X-ray powder diffraction patterns indicated that the products  $\text{Ca}_x\text{Sr}_{1-x}\text{RuO}_3$  ( $x = 0.1, 0.2, 0.3, 0.4,$  and  $0.5$ ) were all single-phase materials, essentially isostructural with the end members of the series and, as there was no evidence of superstructure, they may be assumed to have a random or near-random substitution of Ca for Sr. The patterns were indexed with an orthorhombic unit cell and the resulting cell parameters are listed in Table I. The  $d$ -spacings and relative intensities for the individual phases are deposited with the Editors. As expected, there is a steady decrease in the unit cell volume as  $\text{Sr}^{2+}$  is substituted by the smaller  $\text{Ca}^{2+}$ , but the overall variation is very small indeed. The phase  $\text{Ca}_{0.5}\text{Sr}_{0.5}\text{RuO}_3$  is less distorted than either  $\text{SrRuO}_3$  or  $\text{CaRuO}_3$  and can in fact be indexed with a cubic cell,  $a = 388.53 \pm 0.04$  pm.

TABLE I  
LATTICE PARAMETERS FOR THE  $\text{Ca}_x\text{Sr}_{1-x}\text{RuO}_3$  PEROVSKITE PHASES

Phase	$a$ (pm)	$b$ (pm)	$c$ (pm)	$V$ (nm <sup>3</sup> )
$\text{Ca}_{0.1}\text{Sr}_{0.9}\text{RuO}_3$	552	556	781	0.239
$\text{Ca}_{0.2}\text{Sr}_{0.8}\text{RuO}_3$	551	555	777	0.237
$\text{Ca}_{0.3}\text{Sr}_{0.7}\text{RuO}_3$	550	553	777	0.236
$\text{Ca}_{0.4}\text{Sr}_{0.6}\text{RuO}_3$	549	552	777	0.235
$\text{Ca}_{0.5}\text{Sr}_{0.5}\text{RuO}_3$	548	552	777	0.235
$\text{CaRuO}_3^*$	552.89(3)	535.56(4)	766.01(5)	0.2260
$\text{SrRuO}_3^*$	553.19(6)	557.24(6)	784.96(15)	0.2420

\* Data from Ref. 2.

### Magnetic Susceptibility

Magnetic susceptibility was measured as a function of temperature for all of the solid-solutions, using a Gouy balance. The plots of  $1/\chi_M$  vs  $T$  are shown in Fig. 1.  $\text{SrRuO}_3$  is known to order ferromagnetically below 160°K (3) and substitution of  $\text{Sr}^{2+}$  by  $\text{Ca}^{2+}$  up to  $x = 0.4$  produces a small but regular decrease in the Curie temperature of about 7°K per 10% substitution, indicative of a weakening of the ferromagnetic exchange interaction. For  $\text{Ca}_{0.4}\text{Sr}_{0.6}\text{RuO}_3$  the ordering temperature is still as high as 130°K but the phase  $\text{Ca}_{0.5}\text{Sr}_{0.5}\text{RuO}_3$  deviates markedly in magnetic behaviour from the other members of the series. It does not have a Curie point within the temperature range investigated on the Gouy balance (85–300°K) and extrapolation of the plot of  $1/\chi_M$  vs  $T$  gives an intercept of only 28°K on the temperature axis.

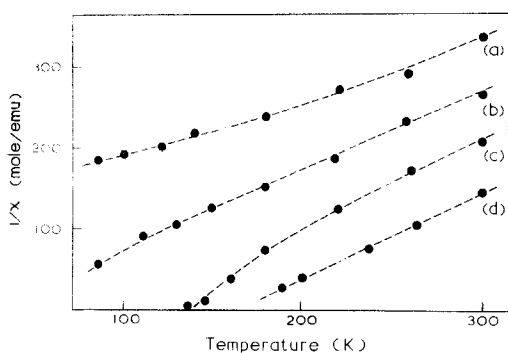


FIG. 1.  $1/\chi_M$  vs  $T$  for (a)  $\text{CaRuO}_3$ , (b)  $\text{Ca}_{0.5}\text{Sr}_{0.5}\text{RuO}_3$ , (c)  $\text{Ca}_{0.4}\text{Sr}_{0.6}\text{RuO}_3$ , and (d)  $\text{SrRuO}_3$ .

In order to determine the Curie temperature of  $\text{Ca}_{0.5}\text{Sr}_{0.5}\text{RuO}_3$  measurements were made down to 4.2°K with a vibrating sample magnetometer. The magnetic behaviour of  $\text{SrRuO}_3$  was similarly studied and the results are shown in Fig. 2 in the form of a plot of spontaneous magnetization (at zero applied field) against temperature. The results confirm the value of 160°K for the Curie temperature of  $\text{SrRuO}_3$  and indicate that  $\text{Ca}_{0.5}\text{Sr}_{0.5}\text{RuO}_3$  orders ferromagnetically at 54°K. Furthermore, the spontaneous magnetization is reduced from 16.78 emu g<sup>-1</sup> for  $\text{SrRuO}_3$  to only 3.2 emu g<sup>-1</sup> for  $\text{Ca}_{0.5}\text{Sr}_{0.5}\text{RuO}_3$  as a result of the weakened ferromagnetic exchange interaction.

As mentioned earlier there is some doubt about the cause of the reduced magnetic moment of  $\text{SrRuO}_3$  (3–5). A possible explanation is that the spins are canted into a spiral. Such a configuration resists reversal more than

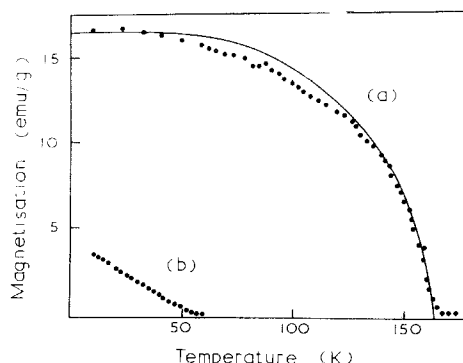


FIG. 2. Plot of magnetization vs temperature for (a)  $\text{SrRuO}_3$  and (b)  $\text{Ca}_{0.5}\text{Sr}_{0.5}\text{RuO}_3$ .

a collinear spin arrangement and would give the low saturation moment and high coercive force which have been observed (3). However, neutron diffraction data (4, 5) have been said to eliminate the spiral structure and to give an estimate for the magnetic moment of  $1.4 \pm 0.4 \mu_B$  at  $4.2^\circ\text{K}$ ; but, only one magnetic peak was available for intensity measurements because the scattering intensities are particularly unfavourable for ruthenium (4). An alternative explanation, based on the observation that the magnetization does not saturate in a flux density of 12.5T at  $4.2^\circ\text{K}$  (where  $\mu_{\text{eff}} = 1.55 \mu_B$ ), attributes the reduced moment ferromagnetism ( $F_R$ ) to partial separation of the spin-up and spin-down bands (4, 5) but again spin-canting would cause a similar effect. Although there is no unambiguous evidence for or against a spiral spin configuration, the possibility should not be excluded, particularly as a similar perovskite,  $\text{SrFeO}_3$ , has a helical antiferromagnetic structure (11), and such arrangements are not uncommon in collective-electron systems.

In order to shed further light on this topic it seemed worthwhile to compare the magnetization behaviour with that expected for an  $S = 1$  spin-state ( $4d^4$  low-spin configuration). The theoretical curve given by the appropriate Brillouin function is shown in Fig. 2 and it can be seen that there is fairly close agreement with the experimental data. This leads us to suggest that there are indeed two unpaired electrons per ruthenium atom and that the reduced moment is probably the result of spin-canting rather than partial overlap of spin-up and spin-down bands.

### Mössbauer Spectra

The Mössbauer spectra of  $\text{CaRuO}_3$  and  $\text{SrRuO}_3$  at  $4.2^\circ\text{K}$  have been published previously (1): that of  $\text{CaRuO}_3$  is a single line appropriate to a paramagnetic Ru(IV) cation on a cubic site, whereas the complex spectrum of  $\text{SrRuO}_3$  can be interpreted as a magnetic hyperfine splitting of the  $\frac{5}{2} \rightarrow \frac{3}{2}$  nuclear transition in  $^{99}\text{Ru}$  with a single hyperfine field of flux density 35.2T (352 kG) and an E2/M1 mixing ratio of  $2.72 \pm 0.17$ .

Spectra for the phase of  $\text{Ca}_x\text{Sr}_{1-x}\text{RuO}_3$  for

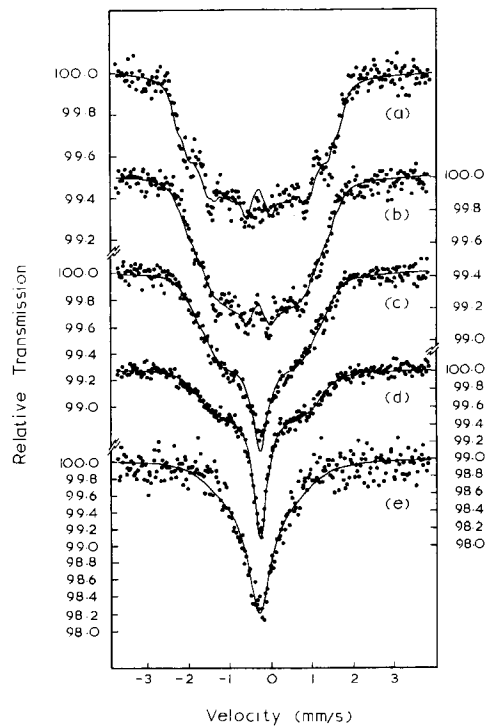


FIG. 3. Ruthenium-99 Mössbauer spectra for the series  $\text{Ca}_x\text{Sr}_{1-x}\text{RuO}_3$ : (a)  $x = 0.1$ , (b)  $x = 0.2$ , (c)  $x = 0.3$ , (d)  $x = 0.4$ , and (e)  $x = 0.5$ .

$x = 0.1, 0.2, 0.3, 0.4,$  and  $0.5$  are shown in Fig. 3. The solid lines through the data are the results of a computer curve-fitting analysis to be described in detail in a later section. It is at once apparent that the spectra are inconsistent with any interpretation based on a single value for the flux density for each composition and attempted computer fits on this basis were very unsatisfactory. For samples with  $x \leq 0.2$  a substantial proportion of the ruthenium nuclei (which decreases as  $x$  increases) experience a magnetic flux density close to 35T, but the inward collapse of the spectrum as  $x$  increases suggests that an increasing proportion experience a smaller flux density. For samples with  $x \geq 0.3$  there is an intense central "paramagnetic" component which increases rapidly with increasing  $x$ . This central portion of the spectrum is anomalously broad for  $x = 0.5$  when compared with the central component for  $x = 0.4$ . These features are unusually complex for a system which is

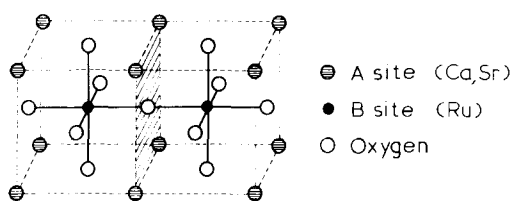


FIG. 4. Two unit cells of the perovskite structure  $\text{ABO}_3$  showing a cube face across which exchange interaction between two ruthenium atoms takes place.

not being magnetically diluted in the conventional sense, and require the development of an electronic model for the system which will serve as a basis for a more quantitative analysis of the data.

In the idealized perovskite lattice each ruthenium atom is coupled by a Ru–O–Ru superexchange to six other ruthenium atoms at the favourable angle of  $\sim 180^\circ$  (see Fig. 4). The intermediate oxygen atoms are in the face centres of a body-centred cube with eight Ca/Sr at the cube corners (*A* sites). Although the shorter Ru–Ru distance in  $\text{CaRuO}_3$  implies a stronger exchange, the oxygen anion orbitals which have a  $p_\pi$ – $d_\pi$  overlap with the ruthenium cations also have a  $p_\sigma$  overlap with four of the *A* cations. The greater electron-pair acceptor strength (Lewis acidity) of the  $\text{Ca}^{2+}$  therefore results in increased competition for the orbitals involved in the superexchange. A similar example can be found in the oxide system  $\text{Ca}_x\text{Sr}_{1-x}\text{MnO}_3$  where increase in calcium content decreases the Néel temperature because the exchange interactions are weakened (12). In each case the chemical influence is more important than either the bond angle distortion or the lattice contraction.

The molecular field theory for localized electrons has been developed by Coey and Sawatzky (13). The magnetic flux density at an  $\text{Fe}^{3+}$  ion, for example, is proportional to the average value of  $\langle S_z \rangle$  which has a strong dependence on the number and strength of the nearest-neighbour interactions. However, in the low-temperature limit,  $\langle S_z \rangle_{T=0}$  tends to the maximum value of the local spin moment so that all  $\text{Fe}^{3+}$  ions, irrespective of the magnetic environment, experience effectively the same flux density. Raising the temperature

causes the flux density to decrease more rapidly for those ions with fewer magnetic neighbours, but a substantial effect is seen only above a reduced temperature of  $T/T_C > 0.2$ . Thus in the spinel  $(\text{Co}_{0.5}\text{Zn}_{0.5})[\text{Fe}_2]\text{O}_4$ , where the number of *A*–*B* exchange linkages is governed by the statistical distribution of Co and Zn, the observed spectrum shows a minimal inward broadening of the  $\text{Fe}^{3+}$  hyperfine splitting at  $90^\circ\text{K}$  ( $T_N = 448^\circ\text{K}$ ) (14). In the present example of  $\text{Ca}_x\text{Sr}_{1-x}\text{RuO}_3$  the temperature of measurement is well below the ordering temperature ( $T_C = 160^\circ\text{K}$  in  $\text{SrRuO}_3$ ) so that, although the substitution of Ca would affect the exchange interactions specifically, no collapse of the hyperfine field would be expected for low Ca content.

Several other factors seem equally unlikely to contribute to the inward collapse of the spectrum. First, the reduction in lattice parameter from  $\sim 554$  pm in  $\text{SrRuO}_3$  to  $\sim 542$  pm in  $\text{CaRuO}_3$  might be expected to cause an increase in the covalency of the Ru–O bonding, but the observed decreases in magnetic flux density are an order of magnitude greater than those found for covalency effects in iron chemistry. Second, it could be argued that the low-spin  $d^4$  ( $S = 1$ ) configuration of the Ru(IV) ion might lead to large orbital and dipolar contributions to the flux density. However, the observed spectra do not seem consistent with this, and similar inward collapse is not seen for example when Fe is substituted for Ru in  $\text{SrRuO}_3$  (15).

A more satisfactory explanation can be proposed on the basis of a collective-electron structure. Although the existence of a finite magnetic moment at a lattice site in a metal can be explained within the overall frame of a collective-electron band model, the theory cannot easily be extended to deal with randomized solid solutions. In particular, little is known about the detailed band structures of these metallic oxides. The behaviour we observe in  $\text{Ca}_x\text{Sr}_{1-x}\text{RuO}_3$  has similarities with the Fe–Al and Fe–Si alloy systems (16, 17). Their structure comprises two interpenetrating simple-cubic lattices, one containing only iron atoms (*A*-sites) and the other containing both iron and aluminium (*D*-sites). The immediate environment of the

*A*-site is eight *D*-sites which form the corners of a cube and which, in ordered Fe<sub>3</sub>Al for example, are occupied by 4Al and 4Fe atoms in an alternant array. The magnetic flux density at the *A*-site is sensitive to the occupation of the *D*-sites and, in the disordered alloys where the *D*-site occupation is random, it has been convincingly shown that the observed flux density at any *A*-site decreases by about 5% per Al in the 8 nearest *D*-sites (about 8% per Si nearest neighbour). However, the flux density is insensitive to the overall Al (or Si) concentration. Furthermore, in disordered Fe<sub>3</sub>Al, ferromagnetic relaxation below the Curie temperature can cause collapse of the hyperfine lines to a "paramagnetic" component from those *A*-sites with more than three aluminium nearest neighbours. The Curie temperature of the ordered Fe<sub>3</sub>Al, where nearly all the *A*-sites have 4Al neighbours, is considerably lower than that of the disordered alloy (18). In these alloys the aluminium is nonmagnetic and causes a weakening of the exchange interactions. In the present instance of Ca<sub>x</sub>Sr<sub>1-x</sub>RuO<sub>3</sub>, the number of interacting nearest neighbours is unaltered, and therefore one must propose that the substitution of Ca has a large effect on the Ru–O–Ru superexchange.

Other metallic systems are also known to feature nearest-neighbour effects. In the Ni–Cu alloys there is evidence that a nickel atom with 8–12 Ni neighbours has an aligned magnetic moment, whereas all those with less than 8 have zero moment (19). Presumably a site which is effectively nonmagnetic is not strongly coupled to the spin-lattice so that fast relaxation results in zero resultant spin moment. Particularly significant is a recent study of Ni–Cu alloys by X-ray photoemission spectroscopy, which shows clearly that the density of states can be represented to a good approximation by superimposing those of the component metals, and that there is only a very limited sharing of electrons by the two constituents, despite the itinerant character of the magnetic electrons (20).

In view of this and other evidence for nearest-neighbour interactions in metallic systems it seems reasonable to assume that the close parallels between the present metallic

oxides and the Fe–Al alloys are not fortuitous. We have, therefore, adopted a simplified phenomenological model which incorporates some of the features of the latter.

### Phenomenological Model

The magnetic field at any given ruthenium atom, Ru<sub>*i*</sub>, will be proportional to  $\langle S_i^z \rangle$  where the maximum value of this average spin-moment is  $S = 1$  corresponding to complete alignment of spin-up and spin-down bands. We shall assume that, in general, the value of  $\langle S_i^z \rangle$  is proportional to the strength of the exchange interactions with the six next-nearest-neighbour ruthenium atoms, Ru<sub>*j*</sub>, so that substitution of Ca for Sr reduces the exchange energy.

The total exchange energy for atom Ru<sub>*i*</sub> including all *j* neighbours will be

$$E = -\sum_j J_{ij} \langle S_i \cdot S_j \rangle$$

where  $S_i$  and  $S_j$  are in units of  $\hbar$  and  $J_{ij}$  is the average exchange integral for the overlapping ions. If  $S_i$  and  $S_j$  are undergoing rapid relaxation then  $\langle S_i \cdot S_j \rangle$  will be zero, but if  $S_i$  and  $S_j$  are strongly coupled then  $E$  will be large and will saturate at low temperatures. To a rough approximation  $E$  will then be proportional to  $\sum_j J_{ij}$ .

As each Ru–O–Ru superexchange takes place through a cube face containing four *A*-site cations (see Fig. 4), we can define the following values for  $J_{ij}$ :

Exchange integral	Geometry	Exchange energy
$J_4$	4Sr on cube face	$4E_1$
$J_3$	3Sr + 1Ca on face	$3E_1 + E_2$
$J_2$	2Sr + 2Ca <i>cis</i> on face	$2E_1 + 2E_2$
$J_2'$	2Sr + 2Ca <i>trans</i> on face	$2E_1 + 2E_2$
$J_1$	1Sr + 3Ca on face	$E_1 + 3E_2$
$J_0$	0Sr + 4Ca on face	$4E_2$

To simplify further, we can also define two energies,  $E_1$  and  $E_2$  ( $E_1 > E_2$ ) so that substitution of Ca for Sr progressively and proportionately changes the strength of  $J_{ij}$ . The magnetic flux density at Ru<sub>*i*</sub> will be proportional to the total moment at the site, and we take this as a linear function of the total

TABLE II  
EXCHANGE INTERACTIONS

Number of Ca nearest-neighbours	Total exchange interaction	Relative probability	Relative exchange energy	Observed magnetic flux density
0	$6J_4$	1	$8E_1$	$B$
1	$3J_4 + 3J_3$	1	$7E_1 + E_2$	$B - \Delta B$
2	$\left\{ \begin{array}{l} 2J_4 + 2J_3 + 2J_2 \\ J_4 + 4J_3 + J_2' \\ 6J_3 \end{array} \right\}$	$\left\{ \begin{array}{l} \frac{3}{7} \\ \frac{3}{7} \\ \frac{1}{7} \end{array} \right\}$	$6E_1 + 2E_2$	$B - 2\Delta B$
3	$\left\{ \begin{array}{l} J_4 + 2J_3 + 2J_2 + J_1 \\ 3J_3 + 2J_2 + J_2' \\ 3J_3 + 3J_2' \end{array} \right\}$	$\left\{ \begin{array}{l} \frac{3}{7} \\ \frac{3}{7} \\ \frac{1}{7} \end{array} \right\}$	$5E_1 + 3E_2$	$B - 3\Delta B$
4	$\left\{ \begin{array}{l} 3J_3 + 3J_1 \\ 2J_3 + 2J_2 + 2J_1 \\ J_4 + 4J_2 + J_0 \\ J_3 + 2J_2 + 2J_2' + J_1 \\ 4J_2 + 2J_2' \\ 6J_2' \end{array} \right\}$	$\left\{ \begin{array}{l} \frac{4}{35} \\ \frac{12}{35} \\ \frac{3}{35} \\ \frac{12}{35} \\ \frac{3}{35} \\ \frac{1}{35} \end{array} \right\}$	$4E_1 + 4E_2$	$B - 4\Delta B$
5	$\left\{ \begin{array}{l} J_3 + 2J_2 + 2J_1 + J_0 \\ 2J_2 + J_2' + 3J_1 \\ 3J_2' + 3J_1 \end{array} \right\}$	$\left\{ \begin{array}{l} \frac{3}{7} \\ \frac{3}{7} \\ \frac{1}{7} \end{array} \right\}$	$3E_1 + 5E_2$	0

exchange energy. This reasoning is intuitive, being essentially true for a simple metal, and hopefully a reasonable approximation in a random solid solution. Although the electrons are itinerant, a change in the local exchange energy is seen directly as a change in the local value of the spin moment.

The random statistical probabilities of the various configurations for calcium substitution on  $A$  sites of up to five strontium atoms are shown in Table II. With the simplifications introduced one finds the very simple result that the observed field at a ruthenium ( $B$ ) site will decrease by a constant increment as the number of calcium neighbours increases. The observation of a "paramagnetic" component for  $x \geq 0.3$  is compatible with a rapid relaxation for weakly coupled atoms. These spectra can only be fitted satisfactorily if it is assumed that only about half of the ruthenium atoms with four calcium neighbours are magnetically coupled. Significantly,  $\frac{10}{35}$  of the ruthenium atoms with four calcium nearest neighbours have at least two exchange interactions through cube faces containing at least three strontium

atoms, which suggests that this may be the criterion for a ruthenium atom to have a coupled spin moment. The criterion is physically realistic in that any given ruthenium atom must be strongly coupled to at least two others to maintain magnetic continuity through the lattice, and we have therefore adopted it in the analysis of all spectra for  $x \geq 0.3$ .

#### Analysis of Mössbauer Data

The solid lines through the Mössbauer data in Fig. 3 were computer curve-fitted on the basis of the foregoing model, assuming a completely random distribution of Ca/Sr cations on the  $A$  sites. The proportion of ruthenium atoms having  $n$  Ca nearest neighbours in  $\text{Ca}_x\text{Sr}_{1-x}\text{RuO}_3$  is then given by the binomial distribution  $8!(1-x)^n x^{8-n} / \{(8-n)! n!\}$ , which yields the percentages listed in Table III.

Ruthenium atoms with 0, 1, 2, and 3 nearest-neighbour calcium atoms were assumed to be magnetically coupled with flux

TABLE III  
PERCENTAGE PROBABILITIES OF SITE OCCUPANCIES

	$x = 0.1$	0.2	0.3	0.4	0.5
$n = 0$	43.0	16.8	5.8	1.7	0.4
1	38.3	33.6	19.8	9.0	3.1
2	14.9	29.4	29.6	20.9	10.9
3	3.3	14.7	25.4	27.9	21.9
4	0.4	4.6	13.6	23.2	27.3
5	—	0.9	4.7	12.3	21.9
6	—	—	1.0	4.1	10.9
7	—	—	0.1	0.8	3.1
8	—	—	—	0.1	0.4
Total which is magnetic	98.8	96.7	88.0	72.1	51.2

densities of  $B$ ,  $B - \Delta B$ ,  $B - 2\Delta B$ , and  $B - 3\Delta B$ , respectively. For  $x = 0.1$  and  $0.2$ , where there is no central component, this procedure gives essentially the same computed value of  $\Delta B$  for  $B = 35.2\text{T}$  (see later), which gives confidence in the analysis. For  $x \geq 0.3$  the proportion of ruthenium atoms having four (or more) calcium neighbours becomes significant (see Table III) and, as stated earlier,  $\frac{1}{3}\frac{6}{5}$  of these are assumed to be magnetically coupled, with a flux density of  $B - 4\Delta B$ , whilst the remaining  $\frac{1}{3}\frac{9}{5}$  and those with 5, 6, 7, and 8 calcium nearest neighbours are assumed to contribute to a central component having a full width at half height of  $0.31\text{ mm s}^{-1}$ . Other models were tried but this was the only one which gave satisfactory fits for  $x = 0.3$  and  $0.4$ .

Because of the troughlike nature of these unresolved hyperfine spectra it was found that the multiple-field fits were not very sensitive to changes in the linewidth of the component lines. The value of  $\Gamma = 0.31\text{ mm s}^{-1}$ , derived for  $x = 0.1$ , was therefore used as a fixed parameter in the final analysis of the spectra for  $x = 0.2, 0.3$ , and  $0.4$ . However, for  $x = 0.5$  a satisfactory fit was obtainable only if the linewidth was allowed to increase. Although there is no direct evidence for partial cation ordering in the samples, this seems to be the most likely cause for the discrepancy in  $\text{Ca}_{0.5}\text{Sr}_{0.5}\text{RuO}_3$  (or  $\text{CaSrRu}_2\text{O}_6$ ). Two further implicit assumptions are that the recoil-free fraction is independent of the nearest-

TABLE IV

PARAMETERS DERIVED FROM CURVE-FITTING<sup>a</sup>  
(CHEMICAL ISOMER SHIFT  $\delta$  RELATIVE TO  
RUTHENIUM METAL AT  $4.2^\circ\text{K}$ )

$x$	$\Delta B/(\text{T})$	$\delta/(\text{mm s}^{-1})$	$\chi^2$	$df$
0.1	$4.90 \pm 0.15$	$-0.314 \pm 0.016$	339	245
0.2	$4.83 \pm 0.15$	$-0.332 \pm 0.008$	325	245
0.3	$4.54 \pm 0.10$	$-0.304 \pm 0.006$	322	245
0.4	$3.72 \pm 0.12$	$-0.303 \pm 0.003$	237	246
0.5	4.9 (fixed) <sup>b</sup>	$-0.324 \pm 0.016$	246	246

<sup>a</sup>  $B$  fixed at  $35.2\text{T}$ ; linewidth fixed at  $0.31\text{ mm s}^{-1}$ .

<sup>b</sup> Linewidth allowed to vary and gave  $0.64 \pm 0.03\text{ mm s}^{-1}$ .

neighbour cations, and that saturation effects can be neglected.

The final fit values are given in Table IV. Taking the spectra for  $0.1 \leq x \leq 0.4$  as a group, these all have the same value for the initial flux density  $B$  and the linewidth so that, apart from the baseline and a normalizing intensity variable, the only free parameters in the final fit are the incremental flux density  $\Delta B$ , and the chemical isomer shift,  $\delta$ . From Table IV it can be seen that the latter is effectively constant within experimental error. It is also apparent that the assumption of a constant value for  $\Delta B$  remains almost within experimental error, except for  $x = 0.4$ , when it is significantly smaller.

This observation of a constant increment in the flux density reduction is good evidence that the local spin moment is caused by the sum effect of the local exchange interactions. This then raises the question as to what effective spin moment the flux density of  $35.2\text{T}$  corresponds to. If it were due to two unpaired  $4d$  electrons on the ruthenium then this would correspond to  $17.6\text{T}$  per electron. In this connection it may be significant that unpublished data on the mixed phase  $\text{SrFe}_{0.5}\text{-Ru}_{0.5}\text{O}_{3-y}$  show a broadened hyperfine field of flux density  $52.9\text{T}$  (15). This phase is an  $\text{Fe}^{3+}\text{Ru}^{5+}$  oxide with a  $^{99}\text{Ru}$  chemical isomer shift of  $+0.116 \pm 0.038\text{ mm s}^{-1}$ . The  $4d^3\text{ Ru}^{5+}$  cation is in some ways comparable to the  $3d^5\text{ Fe}^{3+}$  cation and, as the mixed phase appears to be noncollective this would imply a



flux density of 17.6T per electron in close agreement with the value calculated from the present perovskite phases.  $\text{SrRuO}_3$  therefore has a flux density close to the limit of 35.2T, which would suggest that the spin-up and spin-down bands (i.e., assuming that a metallic description of the ferromagnetism holds) are almost completely separated in this material. The gross reduction in observed magnetic moment can not therefore be caused by band overlap but, as suggested earlier, must arise by a spin-canting mechanism. It should be possible to distinguish conclusively between these two possibilities by measuring the  $^{99}\text{Ru}$  Mössbauer resonance in a large applied magnetic field. Only in the case of  $F_R$  ferromagnetism would an abnormally large augmentation of the flux density be observed. We hope to carry out this experiment at a latter date.

### Acknowledgments

We thank Dr. D. A. Read of the Department of Physics for the use of the vibrating sample magnetometer, and the Science Research Council for financial support and for a maintenance grant (to K.G.S.).

### References

1. T. C. GIBB, R. GREATREX, N. N. GREENWOOD, AND P. KASPI, *J. Chem. Soc. (Dalton Trans.)* 1973, 1253, and references therein.
2. R. J. BOUCHARD AND J. L. GILLSON, *Mater. Res. Bull.* **7**, 873 (1972).
3. A. CALLAGHAN, C. W. MOELLER, AND R. WARD, *Inorg. Chem.* **5**, 1572 (1966).
4. J. M. LONGO, P. M. RACCAH, AND J. B. GOODENOUGH, *J. Appl. Phys.* **39**, 1327 (1968).
5. J. B. GOODENOUGH, *Progr. Solid State Chem.* **5**, 145 (1971).
6. J. B. GOODENOUGH, *Progr. Solid State Chem.* **5**, 330 (1971).
7. J. J. RANDALL AND R. WARD, *J. Amer. Chem. Soc.* **81**, 2629 (1959).
8. P. C. DONAHUE, L. KATZ, AND R. WARD, *Inorg. Chem.* **4**, 306 (1965).
9. J. B. GOODENOUGH, *Progr. Solid State Chem.* **5**, 331 (1971).
10. J. M. LONGO, private communication.
11. T. TAKEDA, Y. YAMAGUCHI, AND H. WATANABE, *J. Phys. Soc. Japan* **33**, 967 (1972).
12. J. A. KAFALAS, N. MENYUK, K. DWIGHT, AND J. M. LONGO, *J. Appl. Phys.* **42**, 1487 (1971).
13. J. M. D. COEY AND G. A. SAWATZKY, *Phys. Status Solidi* **44**, 673 (1971).
14. P. K. IYENGAR AND B. C. BHARGAVA, *Phys. Status Solidi* **46**, 117 (1971).
15. T. C. GIBB, R. GREATREX, N. N. GREENWOOD, AND K. G. SNOWDON, unpublished results.
16. M. B. STEARNS, *J. Appl. Phys.* **35**, 1095 (1964).
17. M. B. STEARNS, *Phys. Rev.* **129**, 1136 (1963).
18. L. CSER, I. DESZI, L. KESZTHELYI, J. OSTANEVICH, AND L. PAL, *Phys. Letters* **19**, 99 (1965).
19. J. PERIER, B. TISSIER, AND R. TOURNIER, *Phys. Rev. Letters* **24**, 313 (1970).
20. S. HUFNER, G. K. WERTHEIM, R. L. COHEN, AND J. H. WERNICK, *Phys. Rev. Letters* **28**, 488 (1972).